JOURNAL OF APPLIED PHYSICS VOLUME 90, NUMBER 1 1 JULY 2001

Role of laser pulse duration and gas pressure in deposition of AlN thin films

Eniko Gyorgy, Carmen Ristoscu, and I. N. Mihailescu[a)]
National Institute for Laser, Plasma and Radiation Physics, Bucharest–Magurele, P. O. Box MG-54, RO-76900, Romania

Argyro Klini, N. Vainos,[b)] and C. Fotakis[c)]
Foundation for Research and Technology – Hellas (FORTH), Institute of Electronic Structure and Laser (IESL), Laser and Application Division, P. O. Box 1527, Heraklion 711 10, Crete, Greece

C. Ghica,[d)] G. Schmerber, and J. Faerber
I.P.C.M.S. (UMR 7504 du CNRS) Groupe ''Surfaces-Interfaces'' 23, rue du Loess 67037 Strasbourg Cedex, France

(Received 20 December 2000; accepted for publication 5 April 2001)

We investigated the relative merits and limits of pulsed laser deposition from AlN targets in vacuum and low-pressure nitrogen in obtaining stoichiometric and crystalline aluminum nitride thin films. We used two UV excimer laser sources ($\lambda = 248$ nm): a nanosecond system ($\tau_{FWHM} = 30$ ns) and, a subpicosecond ($\tau_{FWHM} = 450$ fs) system. The obtained structures were characterized by x-ray diffraction, electron microscopy in cross section, selected area electron diffraction, and profilometry. We demonstrated that the best results are obtained with the sub-ps laser source in vacuum and in low pressure nitrogen when the AlN thin films are very pure, crystalline, clearly exhibiting a tendency to epitaxy. Metallic Al is present in the films deposited with the ns laser source. We believe this is an effect of the gradual decomposition of AlN inside the crater on the target surface under multipulse laser irradiation. © *2001 American Institute of Physics.*
[DOI: 10.1063/1.1376417]

I. INTRODUCTION

The growth of high-quality metal-nitride thin films is of interest because of their very promising applications in high temperature electronics. In particular, aluminum–nitride (AlN) is a wide-band-gap (6.2 eV) III–V semiconductor, which preserves its electrical characteristics (in a *p-n* junction) up to high temperatures (300 °C). Moreover, AlN has a high thermal conductivity (320 W/mK) and a high resistivity (10^{13} Ω cm).[1] For these reasons, AlN is a promising material for microelectronic and optoelectronic devices such as dielectric layers in integrated circuits and high temperature devices.

Several methods have been applied to synthesize and deposit AlN thin films, such as metalorganic chemical vapor deposition (MOCVD),[2–4] ion-beam assisted deposition,[5,6] pulsed laser deposition (PLD), and reactive pulsed laser deposition (RPLD).[1,7–10] Compared to other techniques, PLD and RPLD[11–15] have unique advantages such as: (i) allow the control of the stoichiometry of the deposited material by varying the ambient gas pressure and (ii) due to the use of laser radiation, the amount of impurities in the composition of the deposited material is reduced as compared with other techniques, up to complete elimination.

However, careful investigations have put into evidence a certain excess of metal in the deposited films. The origin of the process causing the dissociation of the nitride molecule and the loss of nitrogen is not yet clearly understood. It can happen either on target or during the transit through vacuum and the cloud of ablated matter. This is in our opinion the effect of the rather prolonged interaction time of every ns laser pulse with the target material and/or with the ablated substance in motion. Accordingly, we assume that a strong decrease of the laser pulse duration should preserve all the other advantages of PLD, and is the most likely factor to prohibit the processes causing the decomposition of AlN molecules. We therefore took advantage of the recent progress of the UV laser facilities generating very short pulses to conduct new experiments for deposition of AlN thin films from bulk AlN targets. In order to eliminate any possible ambiguities, some control experiments have been performed with ns laser pulses in parallel with sub-ps laser pulses under strictly identical irradiation conditions. In view of promoting the formation of crystalline phases we heated the collecting substrate during deposition.

We studied the effect of laser pulse duration (laser intensity), and the nitrogen pressure on the qualities of the deposited AlN films.

II. EXPERIMENT

The experimental setup used for depositions is depicted schematically in Fig. 1. The depositions were performed inside a stainless steel irradiation enclosure. The chamber was first evacuated down to a residual pressure of 10^{-6} Pa. We used AlN high purity targets (99.99%). In order to avoid

[a)]Electronic mail: mihailes@ifin.nipne.ro
[b)]Current address: NHRF-The National Hellenic Research Foundation, Theoretical and Physical Chemistry Institute-TPCI 48, Athens 11635, Athens, Greece.
[c)]Also at Department of Physics, University of Crete, Crete, Greece.
[d)]On leave from the National Institute for Materials Physics, Bucharest-Magurele, P. O. Box MG-7, RO-76900, Romania.

 © 2001 American Institute of Physics

Downloaded 08 Dec 2008 to 194.177.215.121. Redistribution subject to AIP license or copyright; see http://jap.aip.org/jap/copyright.jsp

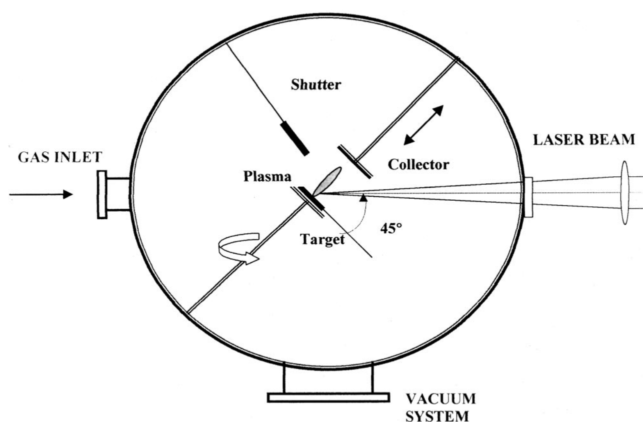

FIG. 1. Experimental setup.

drilling, the AlN samples have been rotated at a frequency of 2 Hz. The laser beam was directed at an incidence angle of 45° with respect to the target surface. For the deposition of one film we applied 10^4 subsequent laser pulses. In the experiments we used two UV KrF* excimer laser sources ($\lambda=248$ nm). The first one, further denoted by laser source A, generated pulses of $\tau_{FWHM}\approx450$ fs duration.[16] The second one is a LAMBDA PHYSIK LPX 200 laser, which emitted pulses of $\tau_{FWHM}\approx30$ ns. We shall further refer to it as laser source B. The laser beams were focused in spots of 0.16 mm^2 in case of laser source A and 3.3 mm^2 in case of laser source B, respectively. The laser fluence was set in all cases at a value of 4 $J\,cm^{-2}$ at the target. Accordingly, the laser pulse intensity is about 8.8×10^{12} $W\,cm^{-2}$ for laser source A and 1.3×10^{8} $W\,cm^{-2}$ for the laser source B. Both laser sources have been operated at a repetition rate of 10 Hz. The laser beam was concentrated on the target using a spherical lens with a 30 cm focal length. Before the depositions the Si ⟨100⟩ collectors were cleaned to remove the native surface oxide layer, with 10% HF solution and then rinsed in distilled water. During the depositions the collectors were heated to 900 °C. In all experiments the target–collector separation distance was fixed at 4 cm. The depositions have been carried out in vacuum (10^{-6} Pa) or in very low dynamic nitrogen pressures of 5×10^{-3}, 5×10^{-2}, and 0.5 Pa. In order to improve targets cleaning a train of 1000 subsequent laser pulses have been directed to the surface of the rotating target while a shutter has been interposed between target and collector. This way the flux of ablated substance containing impurities was prevented access to the collector surface. In view of avoiding any postdeposition contamination, the target and collector were allowed to cool to the room temperature in the ambiance of the deposition gas.

After depositions, the thin films were studied by different complementary surface diagnostic techniques. The thickness and the surface roughness were measured using a Taylor Hobson Leicester talystep.

The crystalline status and the composition of the deposited thin films were studied by x-ray diffraction (XRD). These analyses were conducted with a Siemens Krystaloflex D5000 diffractometer. The investigations were carried out in θ-2θ configuration. The Cu Kα radiation ($\lambda=0.154$ nm) was chosen for excitation.

The crystalline status of the deposited films was also studied by transmission electron microscopy (TEM), using a Topcon EM 002B electron microscope, with a 0.18 nm point resolution operating at 200 kV. For cross-section (XTEM) observation, the specimens have been submitted to mechanical thinning by the tripod method.

III. RESULTS

A. Experiments conducted with the sub picosecond laser source (A)

Typical XRD patterns of the deposited films are given in Figs. 2(a)–2(d). For the films obtained in vacuum [Fig. 2(a)], 5×10^{-3} Pa N_2 [Fig. 2(b)] as well as 5×10^{-2} Pa N_2 [Fig. 2(c)], a unique, very narrow peak at 33° is present in the XRD patterns. This peak is assigned to AlN ⟨100⟩ hexagonal phase. This evidence is consistent with an advanced crystallization status characterized by large crystallites. The intensity of the AlN ⟨100⟩ line increases consistently with the increase of the nitrogen pressure in the deposition chamber. On the other hand, beside the AlN ⟨100⟩ peak, in the XRD pattern of the film deposited at 0.5 Pa N_2 [Fig. 2(d)] a second much smaller unidentified line appears at $2\theta=31.84°$.

We performed XTEM investigations for all deposited samples. Figures 3(a)–3(c) give typical images corresponding to the film obtained at 5×10^{-2} Pa N_2. From Fig. 3(a) we observe a rather uniform film with a thickness of ~50 nm. Direct profilometry recordings are congruent with the results of XTEM studies that the films deposited with the laser source A have a thickness within the 50–100 nm range.

In Fig. 3(b) we give the high-resolution image showing the region of the film close to the interface with the silicon substrate. We noticed not well oriented microcrystals. The crystallite dimensions are no larger than 20 nm. From the interfringe distances on the micrograph, we identified the $(100)h$ planes of the hexagonal AlN phase characterized by an interplanar distance of 0.268 nm [Fig. 3(b)].

The sole presence of AlN within deposited films was confirmed by SAED patterns [Fig. 3(c)]. On the micrograph, the strong spots disposed in a regular bidimensional lattice belong to the Si single-crystal substrate. We indicated by arrows the first three strongest spots of AlN ($100h$, $002h$, $101h$) which appear very weak compared to the Si spots. The *h* index indicates the hexagonal phase.

B. Experiments conducted with the ns laser source (B)

Figure 4 shows the XRD patterns corresponding to the films deposited in vacuum [Fig. 4(a)], 5×10^{-2} Pa N_2 [Fig. 4(b)] and 0.5 Pa N_2 [Fig. 4(c)]. For the film deposited in vacuum [Fig. 4(a)], we observed beside the prevalent AlN ⟨002⟩ peak at 35.8°, two distinct lines corresponding to metallic Al ⟨111⟩ at 38.47° and Al ⟨200⟩ at 44.72°. The AlN orientation in the film changes when making depositions in N_2 at 5×10^{-2} Pa [Fig. 4(b)]. A new prevalent maximum appears at 33° corresponding to hexagonal ⟨100⟩ AlN, while the peak assigned to AlN ⟨002⟩ visible in Fig. 4(a) strongly

Downloaded 08 Dec 2008 to 194.177.215.121. Redistribution subject to AIP license or copyright; see http://jap.aip.org/jap/copyright.jsp

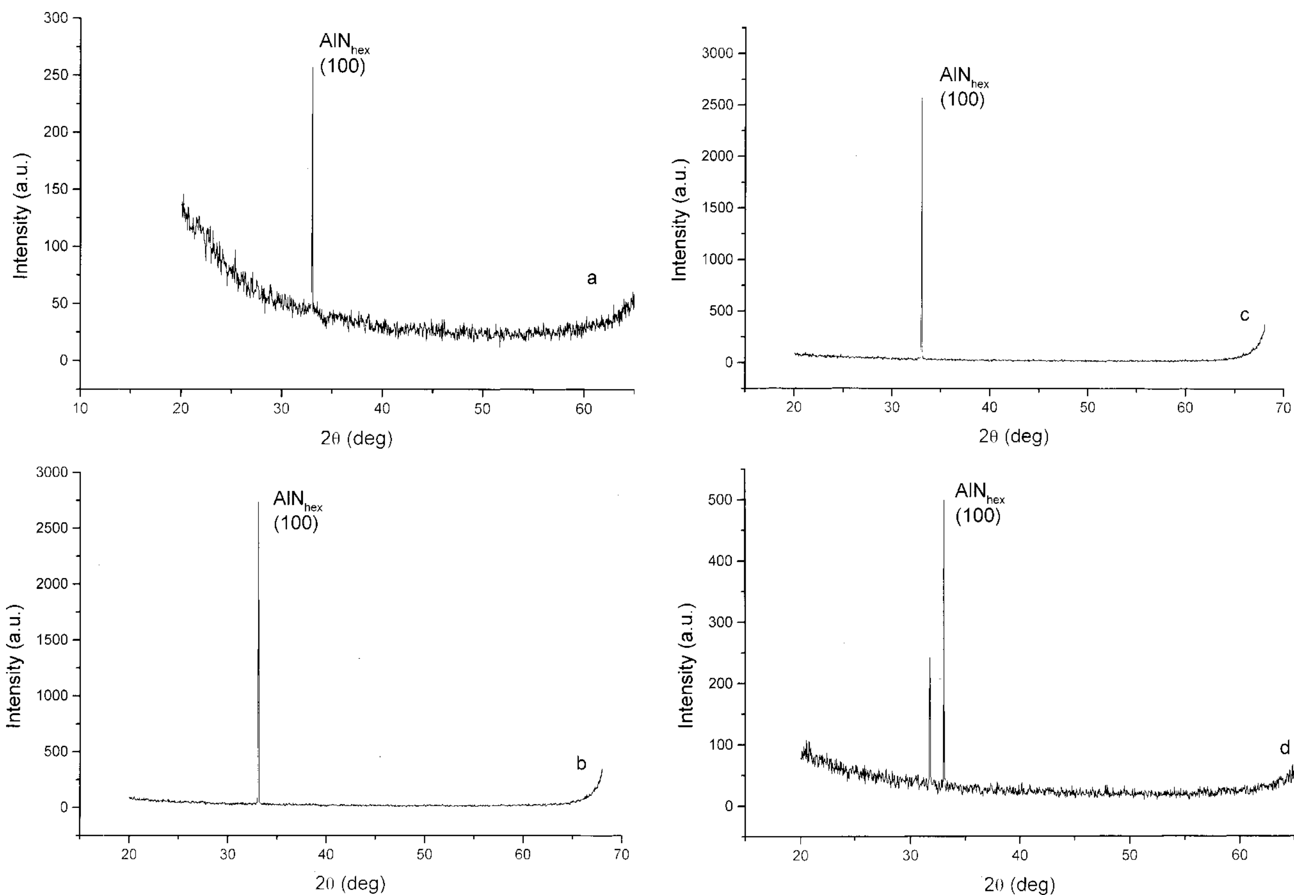

FIG. 2. Typical XRD pattern of the surface of the films deposited from AlN target by multipulse irradiation with laser source A in vacuum (a) and nitrogen at 5×10^{-3} Pa (b), 5×10^{-2} Pa (c), and 0.5 Pa (d).

decreases. Another AlN peak corresponding to the ⟨101⟩ planes becomes evident at 37.9°. When increasing the N_2 pressure, the Al ⟨111⟩ peak at 38.5° is still visible, even if its intensity diminishes. At the same time the Al ⟨200⟩ maximum vanishes [Fig. 4(b)]. The XRD pattern of the film deposited at 0.5 Pa nitrogen [Fig. 4(c)] consists of two peaks corresponding to hexagonal ⟨100⟩ AlN at 33° and hexagonal ⟨002⟩ AlN at 35.8°. We note that at this deposition pressure, the metal phases are completely absent.

As visible from XTEM images, the films are well crystallized, exhibiting a columnar morphology [Figs. 5(a) and 6(a)]. The thickness of the samples is considerably higher than that of the ones deposited with fs lasers in otherwise similar experimental conditions.[17] We notice that in previous experiments[18] the efficiency of laser ablation of AlN was found higher in the nanosecond as compared to the picosecond regime. From the XTEM micrographs we measured a thickness of 700 nm for the film deposited at 5×10^{-2} Pa N_2 [Fig. 5(a)] and 650 nm in the case of the film deposited at 0.5 Pa N_2 [Fig. 6(a)]. These values are congruent with profilometric recordings.

Both samples are highly textured, as can be observed on the corresponding diffraction patterns [Figs. 5(b) and 6(b)]. The diffraction rings are broken into circular segments. As shown by the very intense AlN $(002)h$ spot situated close to (200) Si in Fig. 6(b), a large amount of AlN crystallites have the c axis almost perpendicular to the Si⟨100⟩ substrate. The AlN $(001)h$ planes are more or less parallel to the Si substrate. The high resolution image taken from an area close to the interface [Fig. 6(c)] supports the SAED results [Fig. 6(b)] concerning the AlN crystallites orientations. From the high resolution XTEM image [Fig. 6(c)], one can distinguish the $(002)h$ and $(100)h$ planes of the hexagonal AlN phases, distanced at 0.249 nm and 0.268 nm, respectively. Even after careful examination of the high resolution XTEM image corresponding to the films deposited at 5×10^{-2} Pa or 0.5 Pa ambient N_2 we could not identify any crystal grain or cluster of metallic Al phase.

IV. DISCUSSION

A. Characteristic features of the thin films deposited by PLD with subpicosecond UV laser pulses

The best results we obtained in the deposition of high quality AlN thin films were possible by PLD from AlN targets in low pressure N_2 using the laser source A. Under the best conditions these films were stoichiometric, polycrystalline, and show a tendency of textured growth.

However, at the highest ambient pressure we used in these experiments (0.5 Pa), besides the AlN ⟨100⟩ peak a new line appears. This indicates that the increase of the pressure in the irradiation chamber leads to a variation in the growth direction probably as an effect of increased number of collisions in the gaseous phase. Electron diffraction stud-

Downloaded 08 Dec 2008 to 194.177.215.121. Redistribution subject to AIP license or copyright; see http://jap.aip.org/jap/copyright.jsp

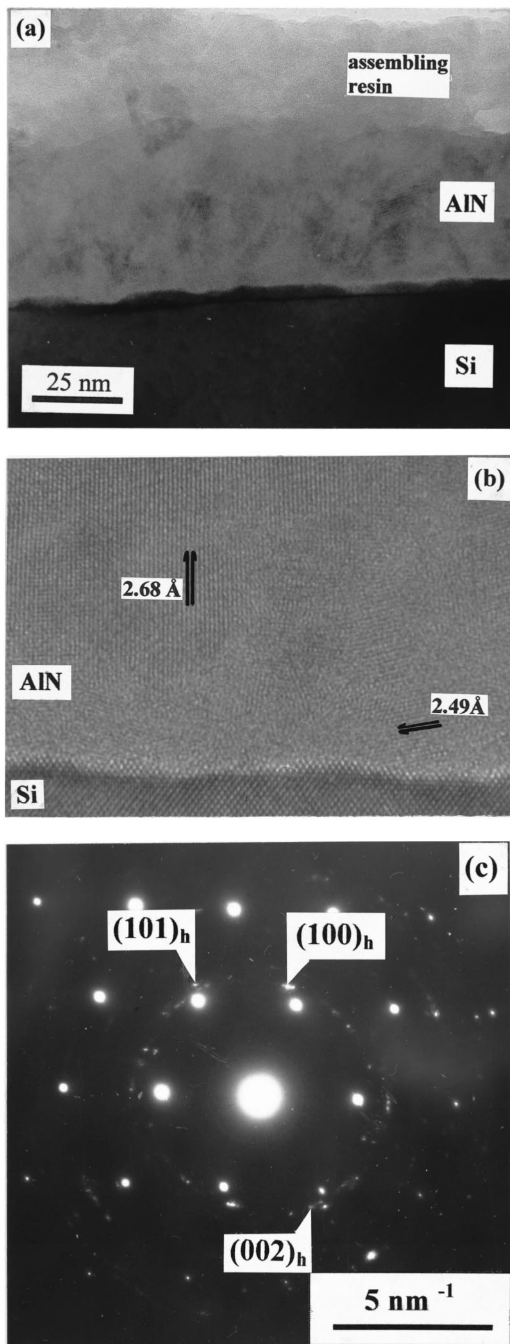

FIG. 3. XTEM images across the films deposited from AlN targets with laser source A in 5×10^{-2} Pa nitrogen (a). Detail recorded in high-resolution (b). The corresponding SAED pattern (c).

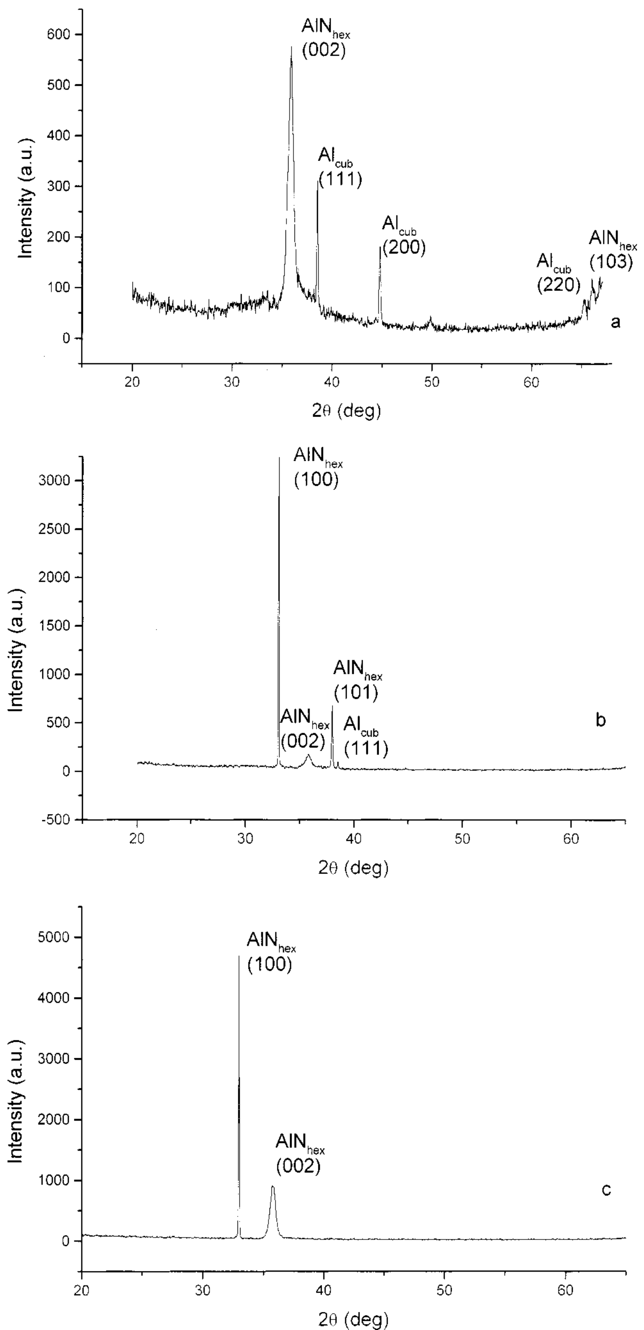

FIG. 4. Typical XRD pattern of the surface of the films deposited from AlN target by multipulse irradiation with laser source B in vacuum (a), and in nitrogen at 5×10^{-2} Pa (b) and 0.5 Pa (c).

ies confirm the presence of AlN crystal grains grown along other directions than ⟨100⟩h with the increase of the gas pressure.

B. Characteristic features of the thin films deposited by PLD with nanosecond UV laser pulses

Quite unexpectedly, the metallic Al phase appeared in XRD spectra of some of the films deposited with the laser source B from AlN targets in vacuum and in low-pressure (5×10^{-2} Pa) nitrogen [Figs. 4(a) and 4(b)]. On the other hand, these spectra contain evidence of more AlN crystallographic orientations than in the case of the patterns of films deposited in the same experimental conditions but with laser source A. We have not yet a definite explanation of the origin of the metallic Al in this case. We can only advance the hypothesis that the multipulse laser irradiation of the target induces a gradual decomposition of the AlN compound in the zones beneath and around the crater. As the laser fluence in our experiments was identical for the laser pulses generated by the sources A and B, we can suppose that the decomposition is the effect of the much larger duration of the heating process in the second case. Indeed, the temporal scale of the laser photons–target substance interaction in-

Downloaded 08 Dec 2008 to 194.177.215.121. Redistribution subject to AIP license or copyright; see http://jap.aip.org/jap/copyright.jsp

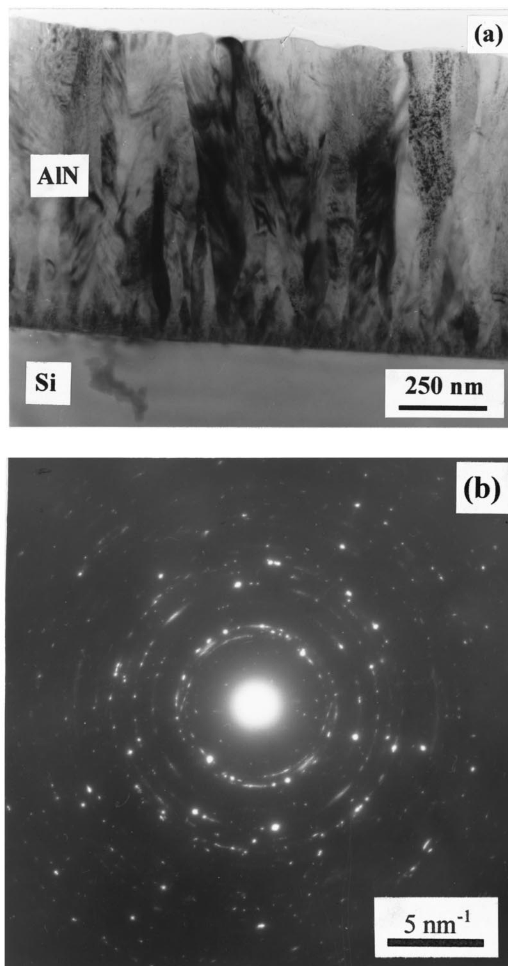

FIG. 5. XTEM images across the films deposited from AlN targets with laser source B in 5×10^{-2} Pa nitrogen (a) and the corresponding SAED pattern (b).

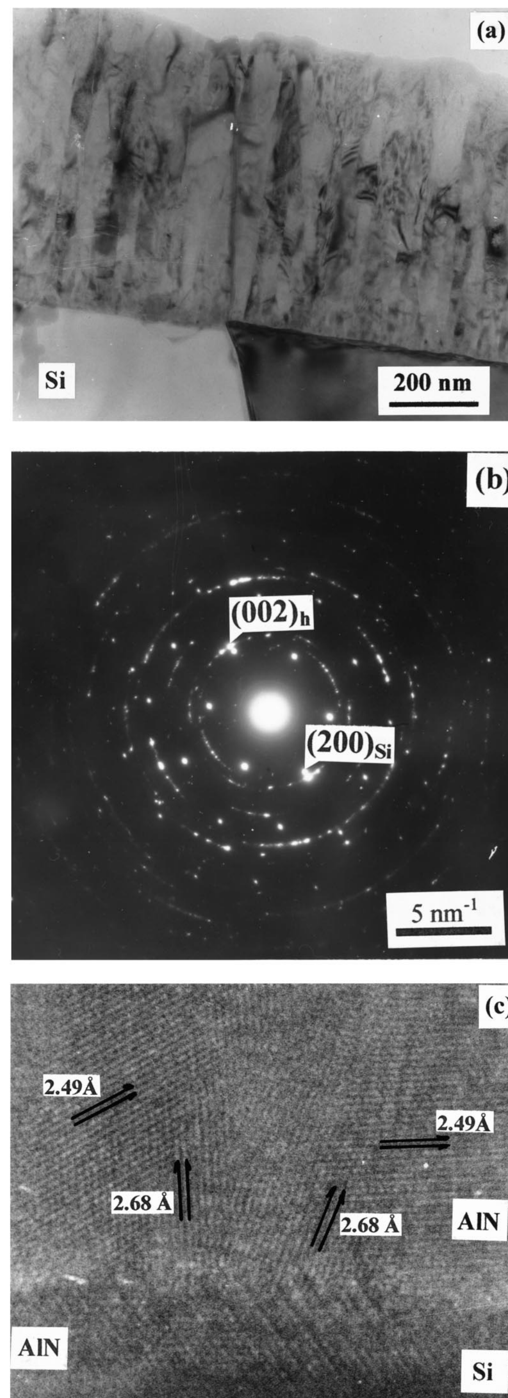

FIG. 6. XTEM images across the films deposited from AlN targets with laser source B in 0.5 Pa nitrogen (a), the corresponding SAED pattern (b), and the high-resolution image taken from an area close to the interface (c).

creases with more than four orders of magnitude in case of the pulses generated by source B, as compared to the laser source A. We note that this effect cannot be considered as resonant because of the large difference between the decomposition energy of AlN, 9 eV, and the energy of photons, 5 eV. On the other hand, reducing the pulse duration, the probability of multiphoton excitation processes increases. The nonlinear absorption increases with laser intensity. We also observed that in case of ablation with long (ns) laser pulses the thermal wave propagates into the irradiated material producing a micrometer-sized melted layer. The evaporation takes the most probably place from the liquid metal, as in conventional thermal evaporation.[19] Thermal evaporation leads to incongruent ablation and the relative concentration of the evaporated species can differ from the original target.[11] Conversely, melting of material in the subpicosecond regime is a nonthermal process.[20,21] Thermal conduction into the target is reduced and the ablation can be considered as a direct transition from solid.[22] This is in our opinion at the origin of the congruent ablation of the AlN target under the action of subpicosecond laser pulses.

Metallization of AlN targets by laser irradiation with ns laser pulses has been observed previously.[23–26] We emphasize that according to Refs. 24–26, even lower fluences ($1.5\ \mathrm{J\,cm^{-2}}$) as compared with that used by us ($4\ \mathrm{J\,cm^{-2}}$) in these new experiments, proved sufficient to induce metallization and melting of the AlN target, because of preferential loss of nitrogen. This behavior represents in our opinion the main shortcoming in using UV lasers with such duration for deposition of pure, good quality AlN thin films. Indeed, in the study performed by Hirayama *et al.*[27] it was shown, that the laser induced thermal decomposition of AlN occurs as an effect of microsecond TEA-CO_2 and nanosecond KrF* exci-

Downloaded 08 Dec 2008 to 194.177.215.121. Redistribution subject to AIP license or copyright; see http://jap.aip.org/jap/copyright.jsp

mer laser irradiation. As a result of the laser induced thermal decomposition process, conductive aluminum lines were directly obtained on the laser treated AlN target surface. In contrast, in the case of femtosecond Ti:sapphire laser irradiation the thermal dissociation process does not occurred and chemical composition of the ablated area remained uncharged. On the other hand, the intensity of the x-ray diffraction peaks corresponding to metallic Al decreases [Figs. 4(a)–4(c)] with the increase of the nitrogen pressure inside the irradiation chamber. These results indicate that the chemical gas–phase reactions during the transit of the ablated material from the target to the collector or the gas–solid reactions on the growing film surface partially compensate the nitrogen loss on the target. It is known from previous experiments, that the interaction of the plume with the reactive gas can contribute to the generation of molecular species required for the growth of the compound nitride.[11]

If, on the other hand, we consider that Al appeared as an effect of AlN decomposition by collisions in gaseous phase, we would have expected more metallic Al at larger gas pressure.

V. CONCLUSIONS

We report the deposition of AlN thin films, under the action of ultrashort (450 fs) UV laser pulses. We also conducted a comparison between the chemical composition of the thin layer obtained from AlN targets by subpicosecond and nanosecond laser irradiation in otherwise identical conditions.

We deposited stoichiometric and epitaxial AlN thin films by PLD from AlN targets using subpicosecond UV ($\lambda = 248$ nm) KrF* laser pulses. The best results have been obtained in vacuum (10^{-5} Pa) and nitrogen at a pressure of 5×10^{-3} Pa and of 5×10^{-2} Pa, when the obtained films entirely consist of highly textured hexagonal ⟨100⟩ AlN.

On the contrary, the films deposited under identical conditions (deposition geometry, laser wavelength, and fluence with ns laser pulses) contained a detectable amount of metallic Al. Metallic Al disappeared only when increasing the gas pressure up to 0.5 Pa, but the crystallographic status of these coatings was quite random. At this stage of our investigations we consider that the metallic Al observed in films was expelled directly from target. We assume that as an effect of the multipulse laser irradiation, AlN gradually decomposes inside the crater. As it follows from our results, the ablation products are mostly AlN molecules, which recondense on the surface of the growing films. We point out that the film obtained by nanosecond laser irradiation of AlN targets in vacuum and 5×10^{-2} Pa N_2, is a mixture of AlN and Al, the hexagonal AlN phase being predominant.

ACKNOWLEDGMENTS

This work was supported by the European Union under the COPERNICUS Contract ''Intereuropean Pulsed Laser Deposition Network For Novel Materials'' (INPULSNET), IC15-CT98-0807. The Romanian co-authors acknowledge the partial support under the Protocol on the Second Session of the Joint Greek-Romanian Commission for S&T Cooperation, 1997–1999, Theme No. 14, ''Reactive Pulsed Laser Deposition of High Quality Thin Films of Metal and Semiconductor Oxides, Nitrides, Carbides and Carbonitrides for Modern Technologies.''

[1] R. D. Vispute, J. Narayan, H. Wu, and K. Jagannadham, J. Appl. Phys. **77**, 4724 (1995), and references therein.
[2] P. Kung, A. Saxler, X. Zhang, D. Walker, T. C. Wang, I. Furguson, and M. Razeghi, Appl. Phys. Lett. **66**, 2958 (1995).
[3] J. Chaudhuri, R. Thokala, J. H. Edgar, and B. S. Sywe, J. Appl. Phys. **77**, 6263 (1995).
[4] K. Ogata, Y. Andoh, S. Sakai, and F. Fujimoto, Nucl. Instrum. Methods Phys. Res. B **59/60**, 22 (1991).
[5] J. Yang, C. Wang, X. Yan, K. Tao, B. Liu, and Y. Fan, Appl. Phys. Lett. **62**, 2790 (1993).
[6] K. Seki, X. Xu, H. Okabe, J. M. Frye, and J. B. Halpern, Appl. Phys. Lett. **60**, 2234 (1992).
[7] T. Ogawa, M. Okamoto, Y. Y. Khin, Y. Mori, A. Hatta, T. Ito, T. Sasaki, and A. Hiraki, Diamond Relat. Mater. **6**, 101 (1997).
[8] A. Giardini Guidoni, A. Mele, T. M. Di Palma, C. Flamini, S. Orlando, and R. Teghil, Thin Solid Films **295**, 7 (1997).
[9] A. Kumar, H. L. Chan, J. J. Weimer, and L. Sanderson, Thin Solid Films **308–309**, 40 (1997).
[10] V. Talyansky, R. D. Vispute, R. Ramesh, R. P. Sharma, T. Venkatesan, Y. X. Li, L. G. Salamanca-Riba, M. C. Wood, R. T. Lareau, K. A. Jones, and A. A. Iliadis, Thin Solid Films **323**, 3 (1998).
[11] *Pulsed Laser Deposition of Thin Films*, edited by D. B. Chrisey and G. K. Hubler (Wiley, New York, 1994).
[12] *Laser Ablation and Desorption*, edited by J. C. Miller (Academic, San Diego, 1998).
[13] I. N. Mihailescu and E. Gyorgy, *Pulsed Laser Deposition: An Overview*, edited by T. Asakura (Springer Series in Optical Science, 1999), pp. 201–214.
[14] N. Chitica, E. Gyorgy, A. Lita, G. Marin, I. N. Mihailescu, D. Pantelica, M. Petrascu, A. Hadgiapostol, C. Grivas, N. Broll, A. Cornet, C. Mirica, and A. Andrei, Thin Solid Films **301**, 71 (1997).
[15] I. N. Mihailescu, E. Gyorgy, G. Marin, M. Popescu, V. S. Teodorescu, J. Van Landuyt, C. Grivas, and A. Hadgiapostolou, J. Vac. Sci. Technol. A **17**, 249 (1999).
[16] S. Szatmari and F. P. Schafer, Opt. Commun. **68**, 196 (1988).
[17] A. Semerok, C. Chaleard, V. Detalle, S. Kocon, J. L. Lacour, P. Manchien, P. Meynadier, C. Nouvellon, P. Palianov, M. Perdrix, G. Petite, and B. Salle, Proc. SPIE **3343**, 1049 (1998).
[18] T. V. Kononenko, S. V. Garnovl, S. M. Klimentov, V. I. Konov, E. N. Loubnin, F. Dausinger, A. Raiber, and C. Taut, Appl. Surf. Sci. **109**, 48 (1997).
[19] D. Bauerle, *Laser Processing and Chemistry* (Springer, Berlin, 1996).
[20] D. von der Linde, K. Sokolowski-Tinten, and J. Bialkowski, Appl. Surf. Sci. **109/110**, 1 (1997).
[21] J. Jasapara, V. V. Nampoothiri, and W. Rudolph, Phys. Rev. B **63**, 045117 (2001).
[22] B. N. Chichkov, C. Momma, S. Nolte, F. von Alvensleben, A. Tünnermann, Appl. Phys. A: Mater. Sci. Process. **63**, 109 (1996).
[23] W. W. Duley, *UV Lasers: Effects and Applications in Materials Science* (University Press, Cambridge, 1996).
[24] H. Esrom, J. Y. Zhang, and A. J. Pedraza, Mater. Res. Soc. Symp. Proc. **236**, 383 (1992).
[25] M. J. DeSilva, A. J. Pedraza, and D. H. Lowndes, J. Mater. Res. **9**, 1019 (1994).
[26] S. Cao, A. J. Pedraza, and L. F. Allard, J. Mater. Res. **10**, 54 (1995).
[27] Y. Hirayama, Y. Hiroyuki, and M. Obara, J. Appl. Phys. **89**, 2943 (2001).

Downloaded 08 Dec 2008 to 194.177.215.121. Redistribution subject to AIP license or copyright; see http://jap.aip.org/jap/copyright.jsp